Research Square

Preprints are preliminary reports that have not undergone peer review.
They should not be considered conclusive, used to inform clinical practice,
or referenced by the media as validated information.

# *From the Canadian Shield to the Andes: A Generative Design Framework for Fractal-Topology Cable Bolts Optimized by Evolutionary Algorithms for Energy Absorption in Deep Hard-Rock Mining and Its Technology Transfer to Peru*

**Paul Ricardo Prudencio Galvez**[1]

pprudencio@autonoma.edu.pe

Universidad Autónoma del Perú https://orcid.org/0009-0000-1986-590X

**Research Article**

**Keywords:** generative design, fractal topology, evolutionary algorithms, cable bolts, energy absorption, rockburst, deep mining, technology transfer, Peru, Canada

**Posted Date:** July 23rd, 2026

**DOI:** https://doi.org/10.21203/rs.3.rs-10441318/v1

**License:** This work is licensed under a Creative Commons Attribution 4.0 International License.
Read Full License

**Additional Declarations:** The authors declare no competing interests.

## Abstract

# Background

deep hard-rock mining in Canada (Sudbury, Timmins, Abitibi, and Kirkland Lake) operates at depths near or beyond 2,500 m, where rockbursts impose dynamic demands that conventional stiff support cannot meet. Canadian and Nordic engineering answered with energy-absorbing elements—cone-type yielding bolts and D-Bolts—showing that dissipation capacity multiplies when the element is designed to deform in a controlled manner. In parallel, the thin-walled structures literature has documented that fractal, hierarchical cross-section topologies raise specific energy absorption at equal mass. No study has yet integrated both research lines for cable bolts or examined their transfer to the Peruvian mining context.

# Methods

a documentary, comparative-analytical study was conducted. First, the published quantitative evidence—each source bearing a verifiable digital identifier—on the static and dynamic performance of conventional and energy-absorbing reinforcement was systematized. Second, a generative design framework was formulated that parameterizes the cable-bolt section through fractal variables (iteration order, scale factor, branching angle, and strand diameter) and optimizes it with the multi-objective evolutionary algorithm NSGA-II coupled to explicit finite-element impact simulation. Third, the mechanical principles underpinning the concept were derived, each with its free-body diagram and governing equations. Fourth, a Canada–Peru technology-transfer matrix was built against representative Peruvian underground operations, detailing machinery, professional profiles, and a training program.

# Results

the documented evidence shows that a 20 mm D-Bolt reaches impact loads of 200–230 kN with 14–20% elongation and cumulative absorption of up to 47 kJ/m, and that a 22 mm × 1.5 m section withstands single 56 kJ impacts—far beyond conventional fully grouted rebar. The Koch-fractal and hierarchical structures literature reports double-digit percentage gains in specific energy absorption at equal mass. The comparative matrix identifies Peru’s concrete gaps in laboratory dynamic testing, high-performance computing for generative design, and specialized talent, and defines a five-phase roadmap for pilots at deepening underground operations such as Cerro Lindo, Yauricocha, and Uchucchacua.

# Conclusions

coupling fractal topology with evolutionary optimization is a plausible, verifiable route to the next generation of energy-absorbing cable bolts. Its transfer to Peru is feasible in stages, provided prototypes are validated through standardized dynamic testing before any operational deployment.

# 1. Introduction

As hard-rock mining migrates to greater depths, in-situ stresses rise and with them the frequency and severity of rockbursts, defined as excavation damage associated with mining-induced seismic events [5, 7, 8]. In Canadian districts such as the Sudbury Basin and the Abitibi belt, several operations work between 2,000 and 3,000 m, a condition under which support must resist dynamic loads and large rock-mass dilation—functions that conventional stiff reinforcement cannot fulfill [5, 7].

The Canadian and Nordic engineering response was the development of yielding, energy-absorbing elements. The modified cone bolt (MCB) dissipates energy through controlled ploughing of the cone through the grout, with field displacements of up to 180 mm reported and a critical sensitivity to bolt–grout bonding [5, 6]. The D-Bolt concentrates plastic deformation in smooth segments between multiple anchors, mobilizing the strength and ductility of the steel along its full length [2, 3]. Systematic reviews of conventional and energy-absorbing rockbolts confirm that dissipation capacity can increase by an order of magnitude when the element is designed to deform in a controlled manner [4]. Cable reinforcement, in turn, offers superior lengths and load capacities for controlling deep wedges and relaxation, within the classical taxonomy of reinforcement systems [1].

In a different field, the mechanics of thin-walled structures has shown that fractal cross-section topologies—Koch curves and self-similar hierarchies inspired by biological structures—substantially raise specific energy absorption (SEA) relative to simple sections of equal mass, thanks to the multiplication of corners and plastic folding paths [10, 11]. Simultaneously, topology optimization and multi-objective evolutionary algorithms, notably NSGA-II, efficiently explore high-dimensional design spaces and produce Pareto fronts of manufacturable solutions, especially when combined with additive manufacturing [9, 12].

# 1.1 Identified gap

The dynamic ground support literature and the fractal energy-absorbing structures literature have evolved in parallel without documented intersection: to the best of the review conducted here, no work (i) applies fractal parameterization to the cross-section and yield elements of cable bolts, (ii) optimizes that parameterization with evolutionary algorithms under simultaneous absorption, mass, and manufacturability objectives, and (iii) analyzes the transfer of such technology from the Canadian benchmark to Andean contexts undergoing progressive mine deepening, such as Peru.

# 1.2 Contribution and scope

This paper contributes: (1) a verifiable quantitative synthesis of the documented performance of the energy-absorbing systems developed and applied in Canadian and Nordic deep mining; (2) the formulation of a fractal–evolutionary generative design framework for cable bolts, with its mechanical principles expressed in free-body diagrams and design equations; (3) a Canada–Peru technology-transfer matrix detailing receiving projects, machinery, professional profiles, and training; and (4) a

phased implementation roadmap. The scope is documentary and propositional: the framework is presented as a verifiable protocol for future experimental research, not as the outcome of tests already performed.

## 2. Materials and methods

# 2.1 Study design

A documentary, comparative-analytical design was adopted in four stages: (S1) systematization of published evidence on energy-absorbing support and fractal structures; (S2) formulation of the generative design framework; (S3) derivation of the mechanical principles and their governing equations; (S4) technology-transfer analysis for Peru through comparative matrices. No laboratory tests or field measurements were carried out; all performance figures come from the cited sources, as indicated in every table and figure.

# 2.2 Sources and inclusion criteria

Articles in indexed journals with a verifiable digital object identifier were included, prioritizing: (i) static and dynamic tests of energy-absorbing bolts with numerical load, displacement, and energy data [2, 3, 4, 6]; (ii) support design principles for burst-prone ground [5, 7, 8]; (iii) the taxonomy of reinforcement systems [1]; (iv) impact performance of Koch-fractal and hierarchical structures [10, 11]; and (v) foundations of multi-objective evolutionary optimization and topology optimization for additive manufacturing [9, 12]. Sources without a verifiable identifier or without traceable quantitative data were excluded.

# 2.3 Proposed generative design framework

The fractal-topology cable bolt (FTCB) is defined by a central load-bearing spine, self-similar branched helices, and discrete yield elements distributed along the tendon (Fig. 1). The cross-section is parameterized with four fractal variables: iteration order n (1–4), scale factor δ (0.25–0.75), branching angle θ (30°–120°), and strand diameter d (6–15.2 mm). Design search is posed as a multi-objective problem: maximize specific energy absorption, minimize mass per meter, and keep the maximum von Mises stress below the limit of the selected steel, under manufacturability constraints. Optimization uses NSGA-II [9], whose non-dominated sorting and diversity preservation suit structural Pareto fronts, coupled to explicit finite-element impact evaluations of every individual in the population (Fig. 4). The compatibility of the approach with metal additive manufacturing of the geometrically complex yield nodes follows documented trends in topology optimization for additive manufacturing [12].

# 2.4 Mechanical formulation and free-body diagrams

The principles governing FTCB performance are derived in Section 3.3, each with its free-body diagram (Fig. 2) and governing equation, following the demand–capacity design logic established for burst-prone ground [5, 7].

## 2.5 Technology-transfer analysis

The Canada–Peru matrix was built by contrasting nine variables (depth, induced seismicity, availability of dynamic support, testing capacity, manufacturing, computing, talent, regulation, and logistics) between the Canadian benchmark and representative Peruvian underground operations, based on the cited evidence and publicly available technical information; depth values are reported as approximate and for reference only.

# 3. Results

## 3.1 The Canadian deep-mining benchmark

Table 1 summarizes the context of the Canadian operations constituting the technological benchmark. The combination of great depth, induced seismicity, and decades of applied research explains why Canada, together with South Africa and the Nordic countries, has led the development of energy-absorbing ground support [5, 7, 8].

Table 1
Canadian benchmark: deep hard-rock underground operations (public technical information, approximate values)

| Operation | District / Province | Commodity | Approx. depth | Relevant geomechanical condition |
|---|---|---|---|---|
| Creighton | Sudbury, Ontario | Ni-Cu | ~ 2.4–2.5 km | High induced seismicity; pioneering use of dynamic support |
| Kidd Creek | Timmins, Ontario | Cu-Zn | ~ 2.9–3.0 km | Among the deepest base-metal mines in the world |
| LaRonde | Abitibi, Quebec | Au | ~ 3.1 km | Sustained deepening with intensive seismic management |
| Macassa | Kirkland Lake, Ontario | Au | ~ 2.2 km | High stresses; yielding support in deep zones |

*Note: reference depths compiled from publicly available technical information; the general geomechanical context of Canadian deep mining is documented in* [5, 7, 8]. *Author's own elaboration.*

## 3.2 Evidence matrix: documented performance of energy-absorbing support

Table 2 and Fig. 3 systematize the published quantitative data. The contrast is sharp: while fully grouted rebar fails at small displacements with limited absorption, the D-Bolt mobilizes the ductility of its entire smooth segment and multiplies the dissipated energy [2, 3, 4].

Table 2
Documented performance of reinforcement elements (data from the cited sources)

| Element | Characteristic load | Displacement / elongation | Energy absorption | Source |
|---|---|---|---|---|
| Fully grouted rebar bolt | High stiffness; load up to steel rupture | Low deformation capacity (tens of mm) | Limited; unsuitable as yielding element | [4] |
| Friction bolt (Split Set) | Low sliding load | Large slip | Moderate, bounded by the low load | [4] |
| MCB cone bolt | Cone ploughing through grout | Up to ~ 180 mm reported in the field | High; sensitive to bolt–grout bonding | [5, 6] |
| D-Bolt, 20 mm | Average impact load 200–230 kN | Elongation 14–20% of length | Up to 47 kJ/m (cumulative, drop tests) | [2] |
| D-Bolt, 22 mm × 1.5 m | Withstands a single 56 kJ impact | Displacement increases linearly with energy | Up to 40 kJ/m (maximum per meter) | [3] |
| Koch / hierarchical fractal thin-walled sections | Increased mean crushing force | Stable progressive plastic folding | Double-digit percentage SEA gains at equal mass | [10, 11] |

*SEA: specific energy absorption. Author's own elaboration from the cited sources.*

# 3.3 Mechanical principles, free-body diagrams, and governing equations

Figure 2. *Free-body diagrams: (a) static axial equilibrium; (b) bond load transfer; (c) dynamic energy balance; (d) plastic work of the deformable segment. Source: author's own elaboration.*

**Principle 1 — Static axial equilibrium (**Fig. 2a**).** The tendon must hold the weight of the potentially unstable block with a static factor of safety. From vertical force equilibrium on the block:

$$T = FS \cdot m \cdot g \; ; \; Tu = \sigma t \cdot As \quad (1)$$

where T is the service tension, m the block mass, g gravitational acceleration, FS the factor of safety, Tu the ultimate tendon capacity, σt the tensile strength of the steel, and As the net steel area. In the FTCB, As is the sum of the central spine and the branched helices of the selected fractal iteration.

**Principle 2 — Bond load transfer (**Fig. 2b**).** Load transfers from the rock mass to the tendon through shear stress at the grout–steel interface. Integrating the bond shear τb over the perimeter:

$$T = \tau b \cdot \pi \cdot d \cdot Lc \rightarrow Lc = Tu / (\tau b \cdot \pi \cdot d) \quad (2)$$

where d is the effective diameter and Lc the critical embedment length. Fractal geometry increases the effective perimeter per unit mass, reducing Lc; the cone-bolt case shows that bonding governs the dissipation mechanism and must be controlled explicitly in design [6].

**Principle 3 — Dynamic energy balance (**Fig. 2c**).** During a seismic event, the ejected block imposes a kinetic-plus-potential energy demand that the system must absorb [5, 7]:

$$E_{dem} = \tfrac{1}{2} \cdot m \cdot (n \cdot ppv)^2 + m \cdot g \cdot \delta_{ult} \leq \Sigma E_{abs} / FSE \quad (3)$$

where ppv is the peak particle velocity, n the ejection-velocity amplification factor, δult the ultimate system displacement, and FSE the energy factor of safety. Eq. (3) formalizes the demand–capacity design criterion for support in burst-prone ground [7].

**Principle 4 — Plastic work of the deformable segment (**Fig. 2d**).** The energy absorbed by the element is the area under its force–displacement curve:

$$E_{abs} = \int F(\delta)\, d\delta \approx F_m \cdot \delta_{ult} \quad (4)$$

and, for smooth segments yielding uniformly, it is proportional to the mobilized steel volume and material properties, a relationship verified experimentally for the D-Bolt [3]:

$$E_{abs} \approx \eta \cdot \sigma_t \cdot \varepsilon_{ult} \cdot V \quad (5)$$

where εult is the ultimate strain, V the volume of the deformable segment, and η an efficiency factor. Eq. (5) is the central lever of the FTCB: fractal topology distributes V into multiple branches yielding in parallel, raising Fm without sacrificing δult.

**Principle 5 — Specific absorption and fractal folding.** Structural merit is measured through specific energy absorption:

$$SEA = E_{abs} / m_b \quad (6)$$

where mb is the element mass. In thin-walled sections, the mean crushing force grows with the number of corners and with fractal order, since each additional corner adds plastic folding lines; Koch and hierarchical structure studies document double-digit percentage SEA gains at equal mass [10, 11]. The optimization problem of the proposed framework is then:

$$\max SEA(n, \delta, \theta, d)\ ;\ \min m_b(n, \delta, \theta, d)\ ;\ \text{s.t. } \sigma_{vM} \leq \sigma_{allow}, \text{manufacturing constraints} \quad (7)$$

solved with NSGA-II [9], which yields the Pareto front of non-dominated designs from which manufacturable candidates are selected.

# 3.4 Canada–Peru technology-transfer matrix

Table 3 contrasts the Canadian benchmark with the Peruvian situation, and Table 4 identifies candidate Peruvian underground operations. Unlike the Canadian Shield—an ancient craton whose seismicity is essentially mining-induced—the Peruvian Andes add subduction-driven tectonic seismicity, which strengthens the case for dynamically capable support even at shallower depths.

Table 3
Canada–Peru comparative matrix for FTCB transfer

| Variable | Canada (benchmark) | Peru (current situation) | Gap and adaptation action |
|---|---|---|---|
| Typical mining depth | 2,000–3,000 m in leading districts | Most operations < 1,500 m, deepening progressively | Prioritize deep, high-stress zones |
| Origin of seismicity | Mining-induced | Induced + subduction tectonics | Design for combined demand (Eq. 3) |
| Dynamic ground support | Yielding bolts and cables in routine use at seismic mines [5, 7] | Incipient adoption; imported elements | Pilots with FTCB and commercial reference elements |
| Laboratory dynamic testing | Established drop-test rigs [3] | No openly accessible certified drop-test facility | Build an impact rig at a university or technology center |
| Manufacturing | Mature forming and additive industry | Wire drawing and forming available; metal AM incipient | Hybrid fabrication: conventional cable + additive yield nodes [12] |
| Computing and generative design | Established HPC and FEM–optimization workflows | HPC capacity concentrated in few universities | University–industry alliances; cloud computing |
| Specialized talent | Geomechanics engineers trained in mining seismicity | Shortage of dynamic-support and optimization specialists | 16-week training program (Table 6) |
| Regulation | Design guidance for burst-prone ground | Safety regulation without a specific rockburst protocol | Technical annex proposal based on demand–capacity [7] |
| Logistics | Local supply chain | High-Andean operations with complex access | Prefabricated modules assembled at the mine surface |

*Author's own elaboration based on the cited evidence and public technical information.*

Table 4
Candidate Peruvian underground operations for FTCB pilots (public technical information, for reference)

| Operation | Region | Commodity | Relevant geomechanical trait | Proposed priority |
|---|---|---|---|---|
| Cerro Lindo | Ica | Cu-Zn-Pb | Longhole stoping with sustained deepening; competent rock mass | High |
| Yauricocha | Lima | Ag-Cu-Zn | Deepening below the main haulage level; rising stresses | High |
| Uchucchacua | Lima | Ag | Deep workings in carbonate rock with high-stress zones | High |
| Inmaculada | Ayacucho | Au-Ag | Narrow veins; dilution control and local stability | Medium |
| Marcapunta (El Brocal) | Pasco | Cu | Expanding bulk underground mining | Medium |
| Poderosa | La Libertad | Au | Deep veins with a record of high local stresses | Medium |

*Prioritization is the author's proposal based on relative depth, deepening plans, and publicly reported stress conditions; it implies no commitment by the operations mentioned.*

## 3.5 Machinery, tools, and materials for implementation in Peru

Table 5
Required equipment by stage (indicative specifications)

| Stage | Equipment / tool | Function | Indicative specification |
|---|---|---|---|
| Characterization | Portable compression press, Schmidt hammer, RQD logging, overcoring cells | Determine UCS, RQD, and in-situ stresses | UCS range 50–250 MPa; ISRM protocols |
| Design | HPC workstation and explicit FEM software + evolutionary optimization library | Run the NSGA-II–FEM workflow (Fig. 4) | ≥ 64 cores, ≥ 256 GB RAM, or cloud computing |
| Manufacturing | Wire drawing and stranding line; metal additive manufacturing cell (laser powder-bed fusion) for yield nodes; heat-treatment furnace | Produce tendons and fractal nodes | High-ductility steel for yielding segments; ±0.1 mm dimensional control on nodes |
| Testing | Instrumented dynamic drop-test rig; universal testing machine ≥ 1,000 kN | Validate Eqs. (3)–(6) on prototypes | Adjustable impact mass and height; energy ≥ 60 kJ |
| Installation | Cable-bolting jumbo with integrated drilling and tensioning; grout injection pump; high-shear mixer | Drilling, insertion, grouting, and tensioning | Boreholes 48–64 mm; controlled water/cement ratio 0.35–0.40 |
| Monitoring | Plate load cells, multipoint extensometers, data acquisition, and microseismic monitoring network | Verify demand and performance in the pilot | Dynamic sampling ≥ 1 kHz during events |

*Author's own elaboration. Commercial brands and models are deliberately omitted; any equipment meeting the functional specification is admissible.*

# 3.6 Professional profiles and training program

Table 6
Professional profiles and proposed 16-week training program

| Profile | Role in the implementation | Key competencies | Training (weeks) |
|---|---|---|---|
| Geomechanics engineer | Characterization, seismic demand, system design (Eq. 3) | Rock mechanics, mining seismicity, rock-mass classification | T1–T4: fundamentals of dynamic ground support [5, 7] |
| Computational design engineer | Fractal parameterization and NSGA-II optimization | Explicit FEM, multi-objective optimization, scientific programming | T1–T4 + P5–P8: FEM–NSGA-II workflow |
| Manufacturing specialist | Production of tendons and yield nodes | Cable forming, metal additive manufacturing, quality control and NDT | P5–P12: fabrication and non-destructive testing |
| Bolting-jumbo operator | FTCB installation at the face | Drilling, grouting, tensioning, safety standards | P9–P12: supervised surface installation |
| Instrumentation technician | Pilot monitoring | Extensometry, load cells, data acquisition | P9–P12: instrumentation and telemetry |
| Safety supervisor | Pilot risk management | Hazard identification, re-entry protocols after seismic events | C13–C16: field phase with re-entry rules |

*T: theory (weeks 1–4); P: practice (weeks 5–12); C: field (weeks 13–16). Program proposed by the author; reference total of 680 contact hours.*

## 3.7 Implementation roadmap

Figure 5 integrates the preceding stages into a five-phase roadmap. The stage-gate criterion is explicit: no prototype proceeds to underground installation without meeting the energy criterion of Eq. (3) on the drop-test rig, replicating the validation practice that underpinned D-Bolt adoption in deep mines [2, 3].

# 4. Discussion

The documentary results converge on three readings. First, the Canadian experience shows that the leap in support capacity came not from stronger steels but from architectures that manage deformation: the D-Bolt multiplies absorbed energy relative to rebar precisely because it redistributes where and how the steel yields [2, 3, 4]. Fractal topology is the natural generalization of that idea: instead of a single smooth segment, a hierarchy of branches yielding in parallel and folding progressively—a mechanism whose effectiveness is documented in thin-walled structures [10, 11]. Second, generative design with NSGA-II turns that intuition into a reproducible procedure: the (n, δ, θ, d) space is too large for manual exploration but tractable for an evolutionary algorithm coupled to explicit simulation [9, 12]. Third, transfer to Peru is not a catalogue import but a capabilities problem: dynamic testing, computing, hybrid manufacturing, and talent, in that order of criticality, as Table 3 reflects.

## 4.1 Public-space applications and the experience of developed countries

The same physics of Equations (3)–(6) governs public-safety problems outside the mine. Developed countries solved the protection of public spaces on slopes—parks, promenades, mountain urban roads—by combining yielding anchors and bolts with flexible rockfall barriers certified through full-scale impact testing, in which cables and dissipators absorb the block's energy exactly as Eq. (4) describes; Switzerland, Japan, Austria, and Italy standardized these tests and their use in public infrastructure. For Peru, a scaled FTCB offers a dual-purpose element: an energy-absorbing anchor for stabilizing the slopes that overlook public spaces in seismic Andean and coastal cities, and a dissipator in protection barriers for roads and lookouts. This duality broadens the industrial base justifying investment in manufacturing and testing, since the same impact rig and the same manufacturing cell serve both mining and resilient public infrastructure.

## 4.2 Limitations

This is a documentary study: the FTCB has not been fabricated or tested, and its target figures (Fig. 3, bar 5) are design goals, not results. The depths and conditions of the cited operations are for reference and may vary. The grout–fractal-node bonding gap (Eq. 2) is the main technical risk identified and must be resolved experimentally before any extrapolation. Finally, the fractal-structure evidence comes from axial crushing of thin-walled sections [10, 11]; its translation to dynamic tension of tendons requires specific validation.

# 5. Conclusions

1. Canadian and Nordic evidence documents that energy-absorbing elements raise support dissipation capacity by roughly an order of magnitude over conventional stiff reinforcement, with verified values of up to 47 kJ/m for the D-Bolt [2, 3, 4].
2. Hierarchical fractal topology, with documented double-digit percentage SEA gains at equal mass [10, 11], and multi-objective evolutionary optimization [9] enable a verifiable generative design framework for the next generation of cable bolts, whose principles are expressed in Equations (1) to (7).
3. Transfer to Peru is feasible in phases if four gaps are closed in order: laboratory dynamic testing, computing capacity for generative design, hybrid manufacturing, and talent development, with pilots prioritized at deepening operations such as Cerro Lindo, Yauricocha, and Uchucchacua.
4. The dual character of the concept—mine support and protection of public spaces on seismic slopes—replicates the route followed by developed countries and strengthens the economic case for investing in national testing and manufacturing capabilities.
5. The future agenda is experimental: prototype fabrication, standardized drop testing, and an instrumented underground pilot confronting the design targets with real measurements.

# Declarations

**Ethics approval and consent to participate:** not applicable. This is a documentary, analytical study involving no human participants, animals, or personal data; it is therefore exempt from ethics committee approval.

**Availability of data and materials:** all data supporting the conclusions come from the cited references, each with a digital object identifier. The comparative matrices produced are available from the corresponding author upon reasonable request.

**Competing interests:** the author declares no competing interests.

**Funding:** this research received no external funding.

**Author contribution:** P.R.P.G. conceived the study, performed the documentary systematization, produced the matrices and figures, and wrote, revised, and approved the final manuscript.

**Figures:** all figures (1 to 5) are the author's own work; copyright © 2026 Paul Ricardo Prudencio Gálvez. No third-party images are reproduced.

# References

1. Windsor CR (1997) Rock reinforcement systems. Int J Rock Mech Min Sci 34(6):919–951. https://doi.org/10.1016/S1365-1609(97)80004-4
2. Li CC (2010) A new energy-absorbing bolt for rock support in high stress rock masses. Int J Rock Mech Min Sci 47(3):396–404. https://doi.org/10.1016/j.ijrmms.2010.01.005
3. Li CC, Doucet C (2012) Performance of D-Bolts under dynamic loading conditions. Rock Mech Rock Eng 45(2):193–204. https://doi.org/10.1007/s00603-011-0202-1
4. Li CC, Stjern G, Myrvang A (2014) A review on the performance of conventional and energy-absorbing rockbolts. J Rock Mech Geotech Eng 6(4):315–327. https://doi.org/10.1016/j.jrmge.2013.12.008
5. Cai M (2013) Principles of rock support in burst-prone ground. Tunn Undergr Space Technol 36:46–56. https://doi.org/10.1016/j.tust.2013.02.003
6. Cai M, Champaigne D (2012) Influence of bolt-grout bonding on MCB conebolt performance. Int J Rock Mech Min Sci 49:165–175. https://doi.org/10.1016/j.ijrmms.2011.11.006
7. Kaiser PK, Cai M (2012) Design of rock support system under rockburst condition. J Rock Mech Geotech Eng 4(3):215–227. https://doi.org/10.3724/SP.J.1235.2012.00215
8. Kabwe E, Wang Y (2015) Review on rockburst theory and types of rock support in rockburst prone mines. Open J Saf Sci Technol 5(4):104–121. https://doi.org/10.4236/ojsst.2015.54013
9. Deb K, Pratap A, Agarwal S, Meyarivan T (2002) A fast and elitist multiobjective genetic algorithm: NSGA-II. IEEE Trans Evol Comput 6(2):182–197. https://doi.org/10.1109/4235.996017

10. Wang J, Zhang Y, He N, Wang CH (2018) Crashworthiness behavior of Koch fractal structures. Mater Design 144:229–244. https://doi.org/10.1016/j.matdes.2018.02.035
11. Zhang Y, Wang J, Wang C, Zeng Y, Chen T (2018) Crashworthiness of bionic fractal hierarchical structures. Mater Design 158:147–159. https://doi.org/10.1016/j.matdes.2018.08.028
12. Liu J, Gaynor AT, Chen S, Kang Z, Suresh K, Takezawa A et al (2018) Current and future trends in topology optimization for additive manufacturing. Struct Multidisciplinary Optim 57(6):2457–2483. https://doi.org/10.1007/s00158-018-1994-3

# Figures

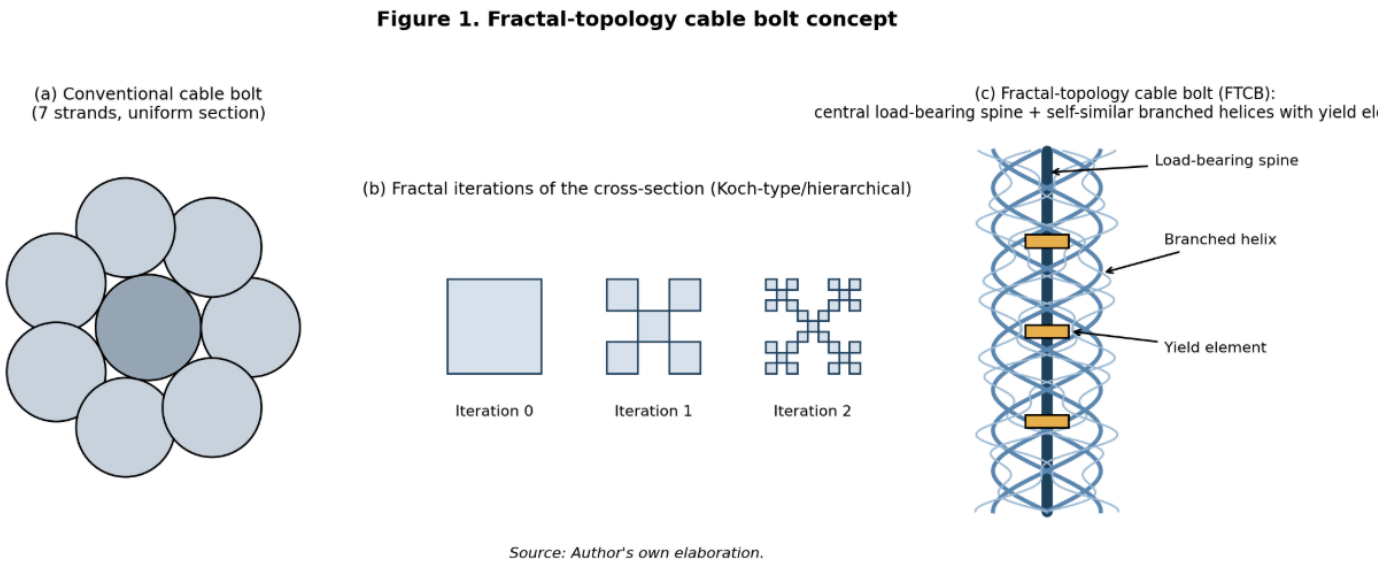
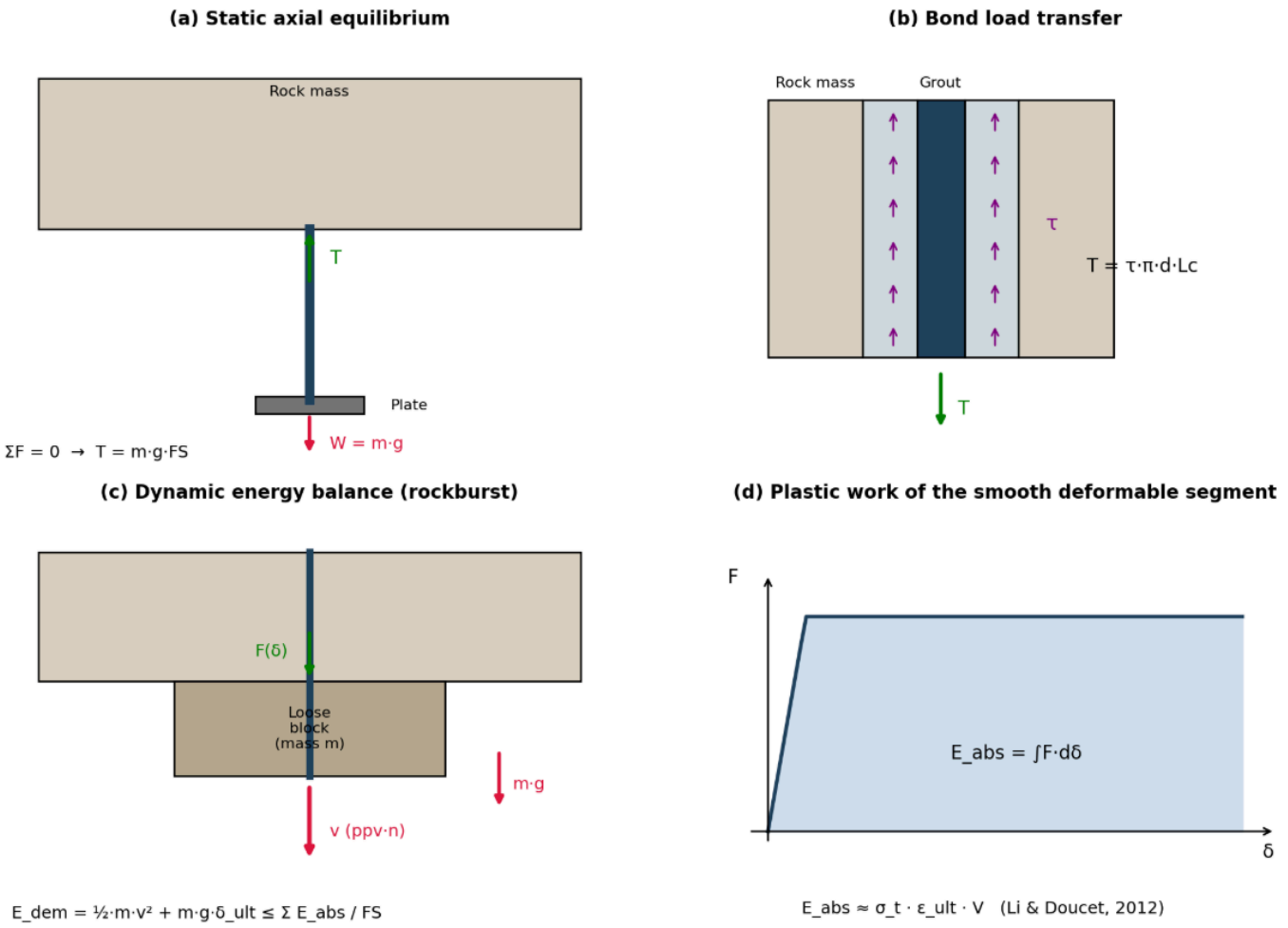


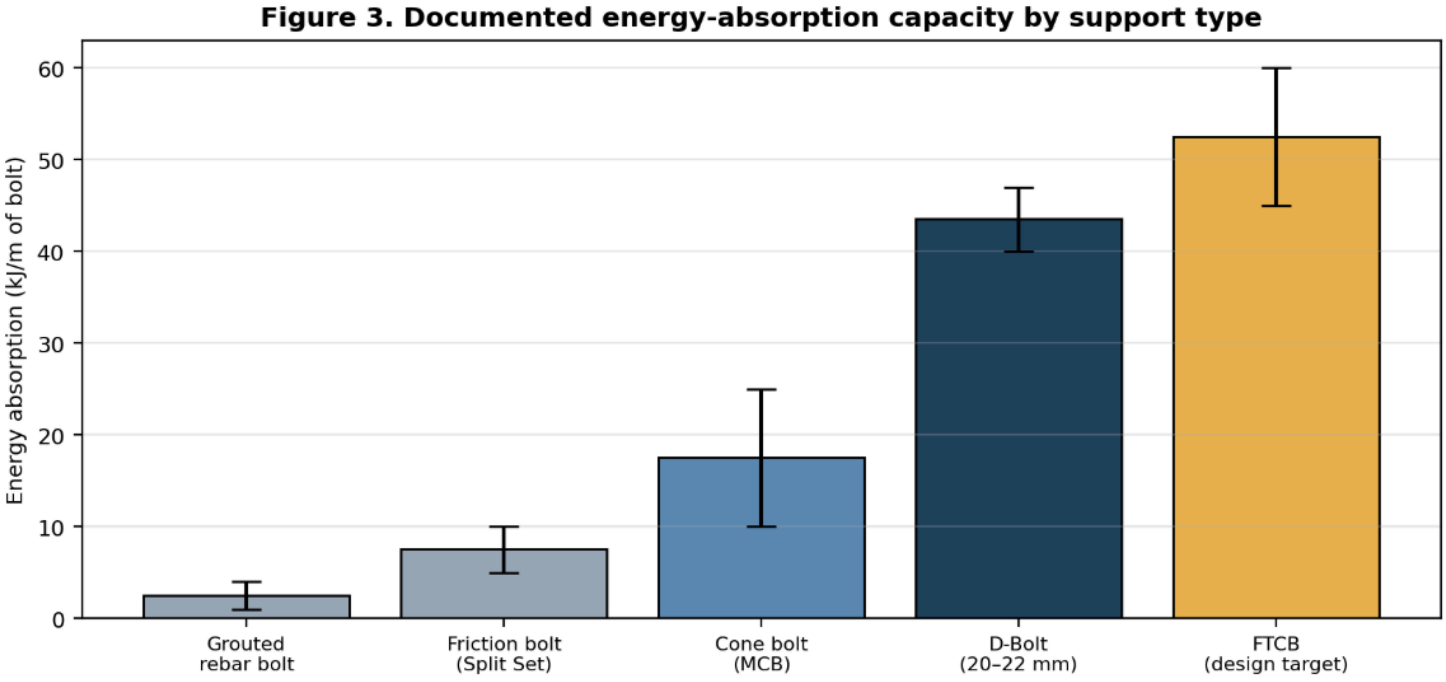

**Figure 1**

*Fractal-topology cable bolt concept: conventional section, fractal iterations of the cross-section, and proposed architecture. Source: author's own elaboration.*



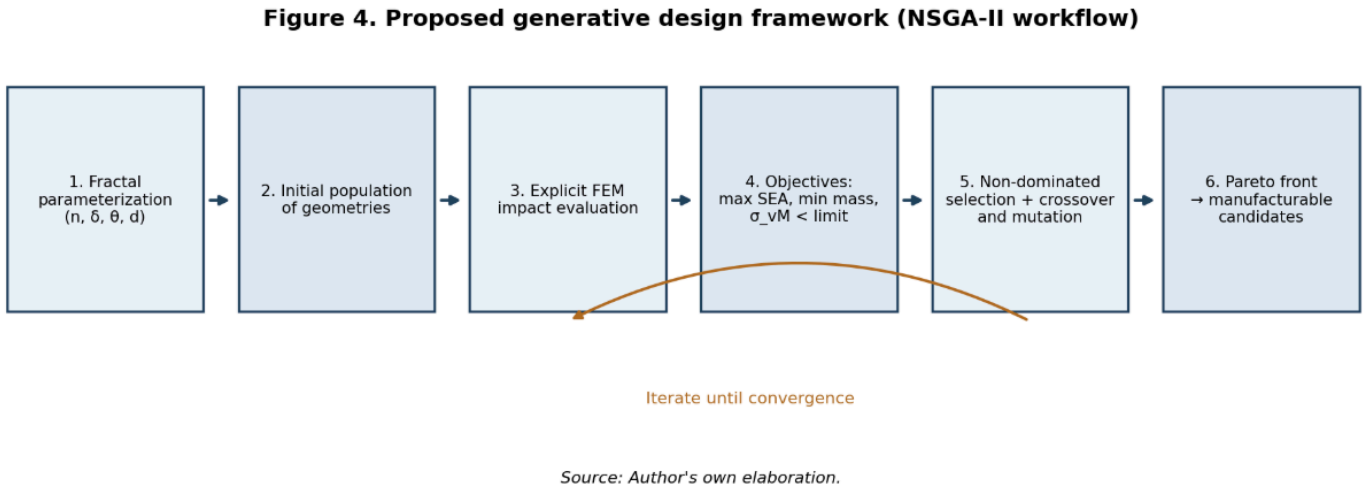

## Figure 2

*Free-body diagrams: (a) static axial equilibrium; (b) bond load transfer; (c) dynamic energy balance; (d) plastic work of the deformable segment. Source: author's own elaboration.*




## Figure 3

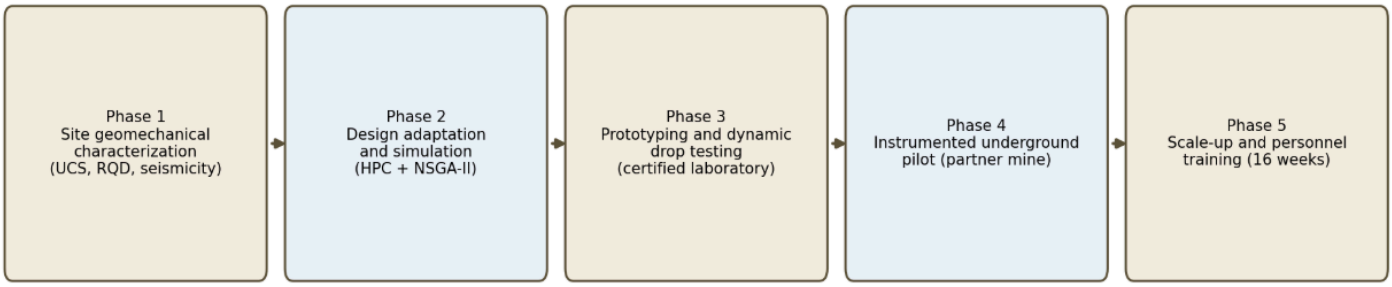
*Documented energy-absorption ranges by support type [2,3,4,6] and FTCB design target (not yet tested). Source: author's own elaboration.*




## Figure 4

*(methodological). Generative design workflow with NSGA-II. Source: author's own elaboration.*

**Figure 5. Proposed implementation roadmap for Peru**




*Source: Author's own elaboration.*

## Figure 5

*Proposed implementation roadmap for Peru. Source: author’s own elaboration.*